Am J Physiol Heart Circ Physiol 313: H548–H557, 2017.
First published June 16, 2017; doi:10.1152/ajpheart.00216.2017.

RESEARCH ARTICLE | *Cardiovascular Neurohormonal Regulation*

A-type K^+ channels contribute to the prorenin increase of firing activity in hypothalamic vasopressin neurosecretory neurons

Soledad Pitra and Javier E. Stern

Department of Physiology, Medical College of Georgia, Augusta University, Augusta, Georgia

Submitted 18 April 2017; accepted in final form 12 June 2017

Pitra S, Stern JE. A-type K^+ channels contribute to the prorenin increase of firing activity in hypothalamic vasopressin neurosecretory neurons. *Am J Physiol Heart Circ Physiol* 313: H548–H557, 2017. First published June 16, 2017; doi:10.1152/ajpheart.00216.2017.—Recent studies have supported an important contribution of prorenin (PR) and its receptor (PRR) to the regulation of hypothalamic, sympathetic, and neurosecretory outflows to the cardiovascular system, including systemic release of vasopressin (VP), both under physiological and cardiovascular disease conditions. Still, the identification of precise cellular mechanisms and neuronal/molecular targets remain unknown. We have recently shown that PRR is expressed in VP neurons and that their activation increases neuronal activity. However, the underlying ionic channel mechanisms are undefined. Here, we performed patch-clamp electrophysiology from identified VP neurons in acute hypothalamic slices obtained from enhanced green fluorescent protein-VP transgenic rats. Voltage-clamp recordings showed that PR inhibited the magnitude of A-type K^+ current (I_A; ~50% at −25 mV), a subthreshold voltage-dependent current that restrains VP firing activity. PR also increased the inactivation rate of I_A and shifted the steady-state voltage-dependent inactivation function toward more hyperpolarized membrane potential (~7 mV shift), thus resulting in less channel availability to be activated at any given membrane potential. PR also inhibited a sustained component of I_A ("window" current). PR-mediated changes in action potential waveform and increased firing activity were occluded when I_A was blocked by 4-aminopyridine. Finally, PR failed to increase superoxide production within the supraoptic nucleus/paraventricular nucleus, and PR excitatory effects persisted in slices treated with the SOD mimetic tempol. Taken together, these experiments indicated that PR excitatory effects on vasopressin neurons involve inhibition of I_A, due, in part, to increases in its voltage-dependent inactivation properties. Moreover, our results indicate that PR effects did not involve an increase in oxidative stress.

NEW & NOTEWORTHY Here, we demonstrate that prorenin/the prorenin receptor is an important signaling unit for the regulation of vasopressin firing activity and, thus, systemic hormonal release. We identified A-type K^+ channels as key molecular targets mediating prorenin stimulation of vasopressin neuronal activity, thus standing as a potential therapeutic target for neurohumoral activation in cardiovascular disease.

prorenin receptor; supraoptic nucleus; K^+ current; superoxide; cardiovascular

ONE OF THE MOST IMPORTANT SYSTEMS involved in cardiovascular and body fluid homeostasis is the renin-angiotensin system (RAS) (12, 17, 38). Despite its well-known systemic functions, it is now well accepted that all components of the RAS are also present within the central nervous system, which, acting independently of the peripheral RAS, can directly influence autonomic and neuroendocrine outflows to the cardiovascular system (8, 16). For example, activation of the brain RAS, involving predominantly ANG II and ANG II type 1 receptors (AT_1Rs), increases sympathoexcitatory outflow and vasopressin (VP) systemic release (24, 35, 42, 53). Despite this evidence, there is still an ongoing debate regarding the localization, sources, cellular targets, and roles of the main RAS components within the brain.

Prorenin (PR) and its receptor (PRR) (19, 32, 41) have recently emerged as two of the most novel players of the brain RAS. Binding of PR to PRR stimulates the catalytic activity of the receptor, converting angiotensinogen to ANG I and ANG II (32, 41). In addition, interaction of PR with PRR initiates intracellular signaling pathways, including MAPK and ERK1/2 (13, 18, 39). Thus, the PR/PRR complex within the brain can mediate both ANG II-dependent and -independent effects.

Recent evidence supports the hypothalamic paraventricular nucleus (PVN) and supraoptic nucleus (SON) as key centers mediating PR/PRR actions. PRR is highly expressed in these nuclei (21, 23, 40), and their activation leads to sympathoexcitation (19) and increased plasma and urine VP levels (41). Moreover, increased PRR expression was reported in the PVN of hypertensive mice, while brain-targeted PRR knockdown decreased blood pressure, sympathetic tone, and plasma VP and VP mRNA levels in these mice (21). Similarly, PRR knockdown in the SON of spontaneously hypertensive rats attenuated hypertension and decreased plasma VP levels (41), and neuron-specific PRR knockout prevented the development of DOCA-salt-induced hypertension, possibly through diminished ANG II formation (22). These studies highlight the importance of the PR/PRR as a novel RAS signaling unit that regulates both sympathoexcitatory outflow and VP release. Still, the precise mechanisms underlying PR/PRR actions in hypothalamic neurons remain largely unknown.

VP release from neurohypophysial axonal terminals is tightly controlled by the degree and pattern of firing activity of VP neurons in the SON/PVN (6). In a recent study, we showed that PRR is highly expressed in VP neurons and that their activation by PR evoked membrane depolarization and increased firing discharge. These effects were ANG II-independent and involved an increase in intracellular Ca^{2+} levels and a Ca^{2+}-dependent inhibition of a voltage-gated K^+ current (34). Thus, our previous studies support that intracellular signaling cascades triggered by PR/PRR, rather than ANG

Address for reprint requests and other correspondence: J. E. Stern, Dept. of Physiology, Medical College of Georgia, Augusta Univ., 1120 15th St., CA-3137, Augusta, GA 30912 (e-mail: jstern@augusta.edu).

II-AT_1R indirect effects, mediate PR actions on VP neurons and VP release. Still, the precise identity of the K^+ channel targeted by PR-PRR in VP neurons remains unidentified.

One of the key intrinsic voltage-gated mechanisms influencing VP neuronal activity is A-type K^+ current (I_A) (5, 28). I_A is a transient, voltage-dependent subthreshold current that restrains firing activity in these neurons (5). Importantly, we have shown that I_A can be inhibited in a Ca^{2+}-dependent manner by relevant neurotransmitters, such as glutamate, leading, in turn, to increased VP neuronal activity (31). Moreover, downregulation of I_A has been associated with increased hypothalamic and brain stem neuronal excitability during hypertension (2, 44, 45). On the basis of all these data, in the present study, we performed patch-clamp electrophysiology in identified VP neurons to test the hypothesis that PR-mediated increased firing discharge involved modulation of I_A.

METHODS

Animals. All procedures were performed in agreement with guidelines of the Augusta University Institutional Animal Care and Use Committee and were approved by the committee. Male heterozygous transgenic enhancle green fluorescent protein (eGFP)-VP Wistar (4–6 wk old, $n = 15$) (51) and Wistar rats (4–6 wk old, $n = 6$) were used. Rats were housed in rooms with a constant temperature of 22–24°C and under a controlled light-dark cycle (12:12 h), with normal rat chow and drinking water available ad libitum.

Slice preparation. Hypothalamic brain slices were prepared according to previously described methods (20). Briefly, rats were anesthetized with pentobarbital sodium (50 mg/kg ip); brains were dissected out, and hypothalamic coronal slices (240 μm) containing the SON/PVN were cut in oxygenated ice-cold artificial cerebrospinal fluid (aCSF) containing (in mM) 119 NaCl, 2.5 KCl, 1 $MgSO_4$, 26 $NaHCO_3$, 1.25 NaH_2PO_4, 20 D-glucose, 0.4 ascorbic acid, 2 $CaCl_2$, and 2 pyruvic acid (pH 7.3, 295 mosmol/kg H_2O). Slices were placed in a holding chamber containing aCSF and kept at room temperature until use.

Electrophysiology. Hypothalamic slices were transferred to a recording chamber and superfused with continuously bubbled (95% O_2-5% CO_2) aCSF (30°C-32°C) at a flow rate of ~3.0 ml/min. Thin-walled (outer diameter: 1.5 mm and innder diameter: 1.17 mm) borosilicate glass (G150TF-3, Warner Instruments, Sarasota, FL) was used to pull patch pipettes (3–5 MΩ) on a horizontal micropipette puller (P-97, Sutter Instruments, Novato, CA). The internal solution contained the following (in mM): 135 potassium gluconate, 0.2 EGTA, 10 HEPES, 10 KCl, 0.9 $MgCl_2$, 4 Mg^{2+}ATP, 0.3 Na^+GTP, and 20 phosphocreatine (Na^+); pH was adjusted to 7.2–7.3 with KOH. Recordings were obtained from neurons with an Axopatch 200B amplifier (Axon Instruments, Foster City, CA) using a combination of fluorescence illumination and infrared differential interference contrast video microscopy. Recordings were obtained from neurons in the SON (15 eGFP and 26 non-eGFP) and the lateral magnocellular subdivision of the PVN (16 eGFP and 2 non-eGFP). Since in our previous study (34) we reported that PR evoked a similar response involving the same mechanism in both eGFP and non-eGFP magnocellular neurosecretory cells from the SON and PVN, data were pooled together for analysis. The voltage output was digitized at 16-bit resolution and 10 kHz and was filtered at 2 kHz (Digidata 1440A, Axon Instruments). Data were discarded if the series resistance were not stable throughout the entire recording (>20% change) (20). Mouse prorenin (2.5 nM, Anaspec) was pressure applied through a picospritzer pipette (5 s, 3 psi).

Current clamp. Mean firing activity and membrane potential (V_m) values were calculated from a 1-min period before drug application and a 1-min period around the peak effect using Clampfit (Axon Instruments) or MiniAnalysis (Synaptosoft) software. The analysis of the action potential (AP) waveform was carried out using APs from these same time periods. APs were aligned at 50% of the rise time, and an averaged AP was obtained and used for quantification using MiniAnalysis (Synaptosoft). To test for the influence of I_A on PR-evoked firing effects, the K^+ channel blocker 4-aminopyridine (4-AP; 5 mM) was used. Since 4-AP facilitates the presynaptic release of neurotransmitters (15), which could mask the direct effects of 4-AP on intrinsic properties, these experiments were performed in the presence of the glutamate and GABA receptors blockers kynurenic acid (5 mM) and picrotoxin (100 μM), respectively.

Voltage clamp. Unless otherwise stated, tetraethylammonium chloride (TEA: 30 mM) and tetrodotoxin (TTX; 0.5 μM) were added to the aCSF for voltage-clamp recordings to block delayed rectifier K^+ channels (IK_{DR}) and Na^+ channels, respectively. The addition of 30 mM TEA involved an equimolar substitution of NaCl (85 mM instead of the original 119 mM). All protocols were run with an output gain of 2 and a Bessel filter of 2 kHz and were leak subtracted (P/4). For activation property experiments, I_A was evoked using depolarizing command steps [−75 to −25 mV, 400 ms, change (Δ) = 5 pA] before and after PR application. The voltage-dependent inactivation properties of I_A were assessed by depolarizing neurons using a command pulse to 0 mV from a series of conditioning steps (−100 to −40 mV, Δ = 5 mV, 300-ms duration) to progressively remove various degrees of I_A inactivation.

ROS assessment. A modified dihydroethidium (DHE) staining method was used to evaluate in the situ production of ROS, as previously described (3). Briefly, coronal sections (16 μm) of hypothalamic frozen tissue containing the SON or PVN were collected on glass slides and equilibrated in fresh aCSF for 10 min in a humidified chamber at 37°C. Slides were then placed in an inverted Zeiss LSM780 confocal microscope stage (atmosphere and temperature controlled), and sections were incubated with DHE (1 μM) in the presence of either aCSF or PR (2.5–5 nM). Immediately after the beginning of incubation, images were acquired every 2 min for a total of 20 min. Zeiss LSM780 software was used for analyses. Forty randomly selected cells per slice were manually traced, and the intensity of fluorescence of each cell was plotted over time. aCSF was used as the vehicle for PR dilution.

Drugs. TTX was purchased from Alomone Laboratories (Jerusalem, Israel). TEA, 4-AP, kynurenic acid, picrotoxin, and 4-hydroxy-TEMPO were purchased from Sigma (St. Louis, MO). DHE was acquired from ThermoFisher Scientific.

Statistical analysis. All values are expressed as means ± SE. Student's paired *t*-tests were used to compare the effects of drug treatment. One- or two-way ANOVA tests with Bonferroni or Dunnett's post hoc tests were used as stated. Differences were considered significant at $P < 0.05$, and n refers to the number of cells. All statistical analyses were conducted using GraphPad Prism (GraphPad Software, San Diego, CA).

RESULTS

Prorenin inhibits the magnitude of I_A in a voltage-dependent manner. Whole cell patch-clamp recordings were obtained in the presence of the Na^+ and K^+ channel blockers TTX (0.5 μM) and TEA (30 mM), respectively. I_A was evoked using depolarizing command steps (−75 to −25 mV, 400 ms, Δ = 5 pA) before and after PR was locally puffed (2.5 nM, 5-s duration) directly onto the recorded neuron. As shown in Fig. 1 and as previously reported (28), I_A in our recording conditions activated at a V_m of −55.6 ± 0.6 mV and displayed a fast rate of activation of 0.5 ± 0.1 ms at a command potential of −25 mV ($n = 9$). After activation, I_A rapidly inactivated,

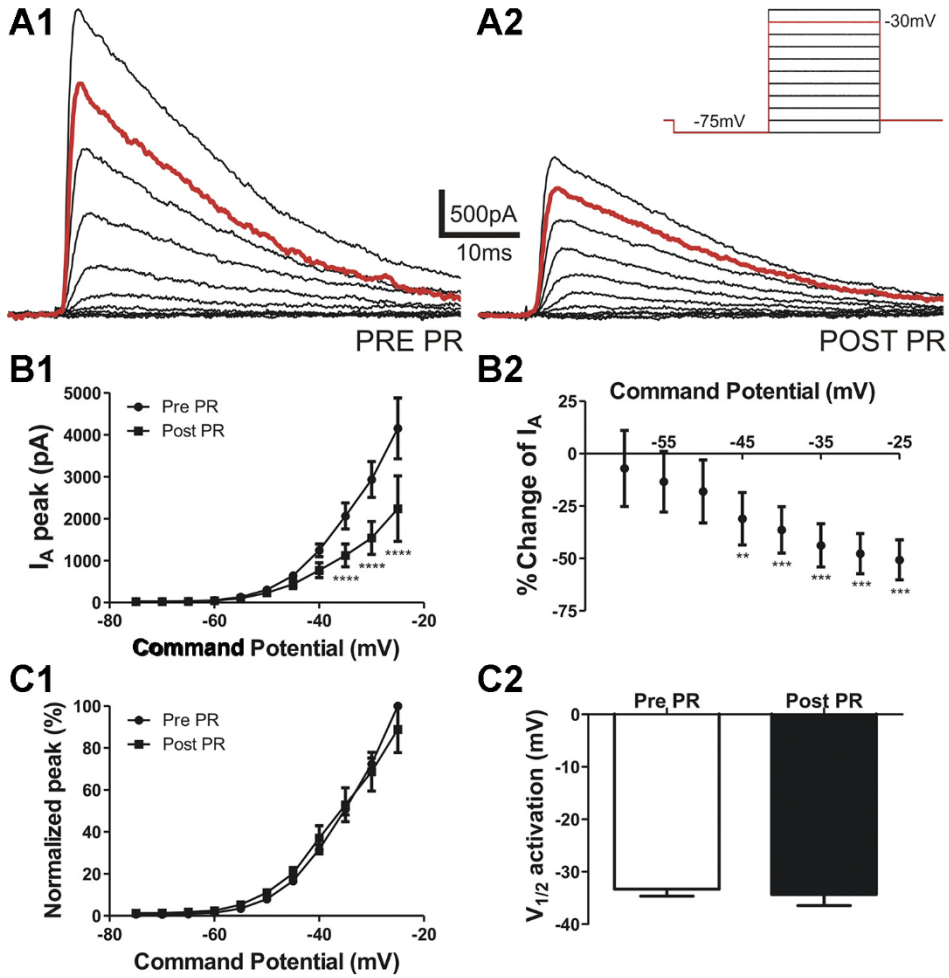

Fig. 1. Prorenin (PR) inhibits A-type K^+ current (I_A) in a voltage-dependent manner. *A*: I_A was activated using depolarizing steps (from −75 to −25 mV in 5-mV increments, 400 ms; *inset*). *A*: representative examples show I_A evoked before (pre; *1*) and after (post; *2*) PR application (5 s). *B*: mean plots of I_A amplitude (*1*) and mean percent inhibition (*2*) after PR exposure versus the command potential (n = 9). Note that the degree of PR-mediated inhibition of I_A amplitude occurred in a voltage-dependent manner, linearly increasing at more depolarized command potentials. *C*,*1*: mean plot of normalized I_A amplitude versus command potential before and after PR. Individual plots were fitted with a Boltzmann function to obtain the mean half-activation potential ($V_{½}$) values shown in *C*,*2*. Note that PR had no effect on I_A $V_{½}$ of these neurons. ****P < 0.0001 vs. respective pre-PR by two-way repeated-measures ANOVA followed by Bonferroni multiple comparisons; **P < 0.01 and ***P < 0.001 vs. the percent change at −60 mV by one-way repeated-measures ANOVA followed by Dunnett's multiple-comparison test.

displaying a monoexponential decay [inactivation time constant (τ): 15.8 ± 1.6 ms at a command potential of −25 mV].

The magnitude of I_A was significantly inhibited after PR exposure (two-way ANOVA = PR × V_m, F_{V_m}: 16.8, P < 0.0001, and F_{PR}: 68.2, P < 0.0001; interaction: F = 13.1, P < 0.0001; Fig. 1*B1*). Importantly, the degree of I_A inhibition by PR was voltage dependent (P < 0.0001, one-way ANOVA; Fig. 1*B*,*2*), with the degree of inhibition increasing in a linear manner as a function of the depolarizing command step (r^2 = 0.99, P < 0.0001).

To determine whether PR affected the voltage-dependent activation properties of I_A, we generated mean normalized current-voltage plots, which were fit with a Boltzmann function to calculate the half-activation potential ($V_{½}$). As shown in Fig. 1*C*,*1* and *2*, PR did not affect the voltage-dependent activation properties of I_A (n = 8, P > 0.6).

Finally, the rate of activation of I_A was not significantly different before and after PR (P > 0.3, Fig. 2*A*,*1* and *2*).

Prorenin effects involve changes in I_A inactivation properties. After activation, I_A is known to rapidly inactivate. We examined the rate of inactivation by fitting a monoexponential function to the decay phase of I_A after a voltage command to −25 mV, and we determined τ. As shown in Fig. 2*B*,*2*, the rate of inactivation of I_A was significantly faster (i.e., smaller τ) after PR application (n = 8, P < 0.05).

Another functionally relevant property of I_A is voltage-dependent, steady-state inactivation, which determines the number of available channels to be activated at any given V_m (28). To establish whether PR affected the voltage-dependent inactivation properties of I_A, neurons were depolarized using a command pulse to 0 mV from a series of conditioning steps (−100 to −40 mV, Δ = 5 mV, 300-ms duration), with the aim of progressively removing various degrees of I_A inactivation. Plots of normalized currents as a function of the conditioning step were generated and fit with a Boltzmann function to calculate the half-inactivation potential. As shown in Fig. 3, PR shifted the voltage dependence of inactivation of I_A toward a more hyperpolarized V_m (leftward shift), which was reflected as a significant hyperpolarization of half-inactivation potential (n = 11, P < 0.005; Fig. 3*B*,*3*). This is indicative of a higher degree of I_A inactivation at any given V_m, standing, in turn, as a factor that contributes to the smaller evoked I_A magnitude in the presence of PR.

To gain more insight into the contribution of steady-state inactivation to the overall inhibitory effect of PR on I_A magnitude, we repeated the activation protocols as shown in Fig. 1 but tested PR effects while holding neurons at a more hyperpolarized holding voltage (−100 instead of −75 mV) to completely remove basal, steady-state I_A inactivation before the depolarizing command step. We found that PR inhibitory

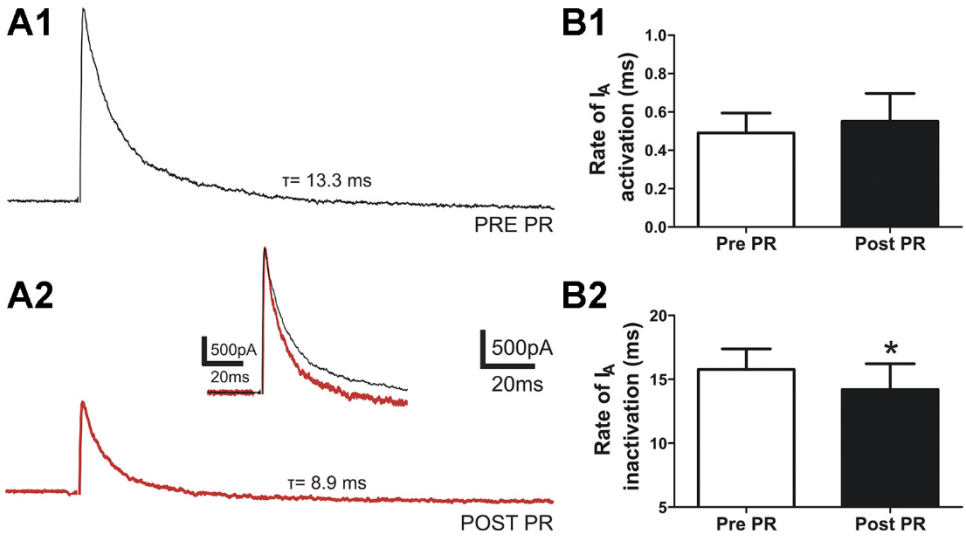

Fig. 2. PR effects on I_A activation and inactivation rates. *A*: representative traces of I_A elicited by a depolarizing command step to −25 mV from a holding potential of −75 mV before (*1*) and after (*2*) PR. The *inset* shows both traces superimposed and scaled to better depict changes in I_A kinetics. Note that after PR (red trace) the I_A activation rate was not affected, while the rate of inactivation was faster. *B*: mean summary data showing no significant differences in the activation rate ($n = 8$, $P > 0.3$; *1*) but a significantly faster inactivation rate [inactivation time constant (τ), $n = 8$; *2*). *$P < 0.05$ vs. pre-PR using Student's paired *t*-test.

effects on I_A were significantly diminished (by ~70%, $n = 8$) compared with those cases in which I_A was evoked from a −75-mV holding potential (−75-mV holding potential: 47.7 ± 9.6% inhibition and −100-mV holding potential: −8.9 ± 6.7% inhibition, $P < 0.01$) after a command step to −30 mV. These results suggest that an enhanced steady-state inactivation of I_A plays an important role in mediating the overall inhibitory effect of PR on I_A magnitude.

Prorenin inhibits I_A window current. Superimposing the normalized steady-state voltage-dependent activation and inactivation curves revealed the presence of an overlapping area near resting V_m, thus supporting the existence of a "window current" (Fig. 4*A*) (7, 30, 46). We found that after PR application, I_A window current was significantly shifted toward more hyperpolarized potentials, from an initial range of −75.6 to −56.4 mV and −80.6 to −65.0 mV after PR ($n = 9$, Fig. 4*C*). The window current peak before PR was also significantly shifted toward more hyperpolarized potentials, from an initial V_m of −61.4 ± 2.1 to −67.2 ± 2.7 mV after PR ($P < 0.005$). Finally, the magnitude of the window current range was also

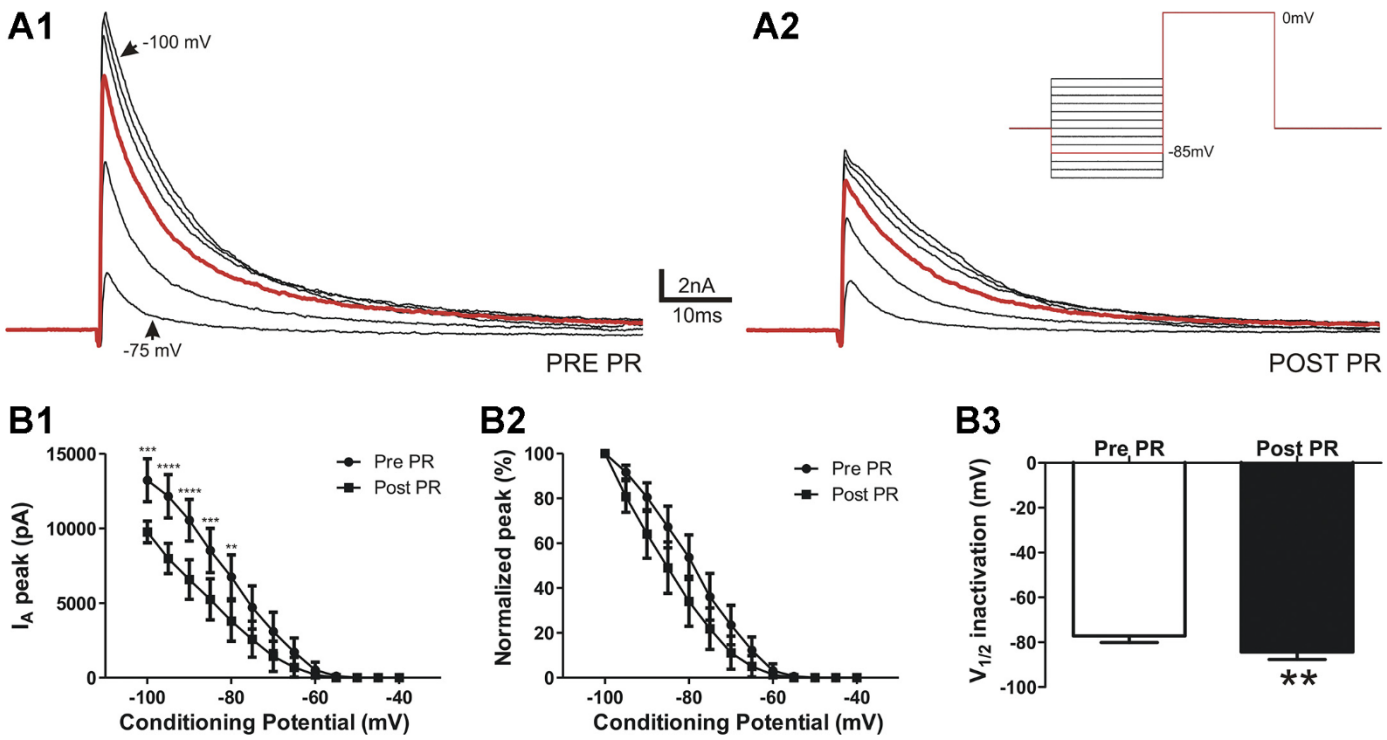

Fig. 3. PR increases I_A steady-state voltage-dependent inactivation properties. *A*: representative example of I_A evoked by a voltage command step to 0 mV from conditioning steps between −100 and −40 mV (*inset*) before (*1*) and after PR (*2*). *B*: plots of mean I_A amplitude (*1*) and normalized I_A amplitude versus the variable inactivating conditioning potential (*2*). Note that PR caused a hyperpolarizing shift on the steady-state inactivation curve. *B*,*3*: mean I_A $V_{½}$ before and after PR application ($n = 11$). **$P < 0.01$, ***$P < 0.001$, and ****$P < 0.0001$ vs. respective pre-PR using two-way repeated-measures ANOVA followed by Bonferroni multiple comparisons; **$P < 0.01$ vs. pre-PR using Student's paired *t*-test.

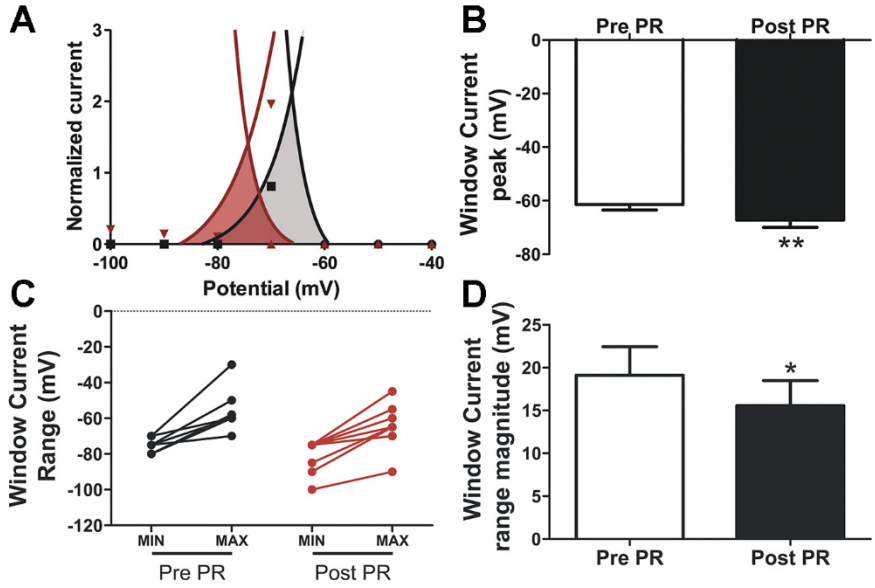

Fig. 4. PR affects I_A window current. *A*: representative example of one neuron showing that combining the mean normalized steady-state activation and inactivation plots revealed an area of overlap (I_A window current, shaded areas). Note that after PR (red), both the peak (i.e., the voltage at which the curves intersect; *B*) and the whole voltage range of the window current (*C*) shifted to more hyperpolarized levels. Moreover, the magnitude of the window current voltage range was significantly narrower after PR (*D*). *$P < 0.05$ and **$P < 0.01$ vs. pre-PR ($n = 9$) using Student's paired *t*-test.

significantly diminished after PR (mean range amplitude: 19.1 ± 3.3 mV before PR vs. 15.6 ± 2.9 mV after PR, $n = 9$, $P < 0.05$). This hyperpolarizing shift along with the narrowing of the voltage range thus resulted in an almost complete absence of the window current around the typical resting V_m of magnocellular neurosecretory neurons (i.e., −65 to −60 mV) (1, 28, 47) after PR, an effect expected to result in membrane depolarization and increased firing discharge.

Prorenin inhibition of I_A increases neuronal firing activity and affects AP properties. We previously reported that focal application of PR stimulates firing activity of VP neurons (34). On the basis of our current results showing that PR inhibits I_A, we repeated current-clamp experiments in the presence of the K^+ channel blocker 4-AP to determine the contribution of I_A to this effect. Given our previous results showing a very slow or lack of recovery after a single PR application (34), experiments were performed in separate neurons preincubated in either control aCSF or 5 mM 4-AP, a concentration known to more specifically inhibit I_A over other voltage-gated K^+ currents (46). As shown in Fig. 5, PR focal application induced a significant increase in firing discharge in normal aCSF ($n = 9$, $P < 0.001$). Conversely, this effect was completely absent in neurons preincubated in 4-AP ($n = 11$, $P > 0.6$).

Since I_A is known to influence the AP waveform in hypothalamic neurons (14, 28, 46), we also monitored the effects of PR on the latter. We found that PR increased the AP half-width, prolonged the AP decay time course, and reduced the hyperpolarizing afterpotential peak under normal conditions (Table 1 and Fig. 5*C*,*1*–*3*). These changes were abolished when the same experiments were carried out in the presence of 4-AP (Table 1 and Fig. 5*C*,*3*).

ROS production is not involved in mediating PR actions. To attempt to identify the potential mechanism underlying PR-mediated I_A inhibition, and on the basis of previous studies that link ROS production with neuron excitability and I_A modulation (27, 50, 54), we repeated current-clamp experiments in the presence of the SOD mimetic tempol (5 mM), a concentration previously shown to efficiently act as a ROS scavenger in brain slices (26). PR excitatory effect persisted in the presence of tempol ($n = 10$, $P < 0.001$; Fig. 6), and the magnitude of this effect was not significantly different from that observed in control aCSF ($P > 0.2$), suggesting that ROS formation is not a critical mechanism involved in PR excitatory effects on SON/PVN neurons.

To further confirm these results, DHE staining was used to measure the in situ production of ROS in PVN and SON slices ($n = 8$ and 2, respectively) after PR application. Tests were run in pairs: one slice was incubated with aCSF alone and another slice was incubated in the presence of PR (2.5–5 nM). As previously reported, there was a progressive increase in background DHE fluorescence levels during imaging acquisition, even in the presence of regular aCSF (3, 55). Thus, to quantify the effect of PR, we calculated proportional changes in DHE staining fluorescence intensity (normalized by aCSF) at each particular time point and plotted this proportional change over time. We found that DHE staining within the SON/PVN did not change in the presence of PR compared with the respective aCSF control ($F = 0.53$, $P > 0.8$ by one-way ANOVA; Fig. 6). A positive control was carried out using ANG II instead of PR, which has been previously shown to efficiently increase ROS production using the same approach (3). Taken together, these results argue against a contribution of oxidative stress as a mechanism underlying PR excitatory effects on VP neurons.

DISCUSSION

In a recent study, we showed that PR stimulates the firing discharge of hypothalamic VP and presympathetic neurons through distinct ANG II-independent and -dependent mechanisms, respectively (34). PR effects on both cell types, however, involved binding of PR to PRR and the inhibition of a voltage-gated K^+ channel in a Ca^{2+}-dependent manner. Here, we focused on SON/PVN magnocellular neurosecretory cells, including a subpopulation of identified VP neurons, which are a major target of the central RAS (29), to further elucidate the specific cellular mechanisms by which PR/PRR modulates their activity and, ultimately, hormonal output and fluid/electrolyte homeostasis. Results from the present work provide

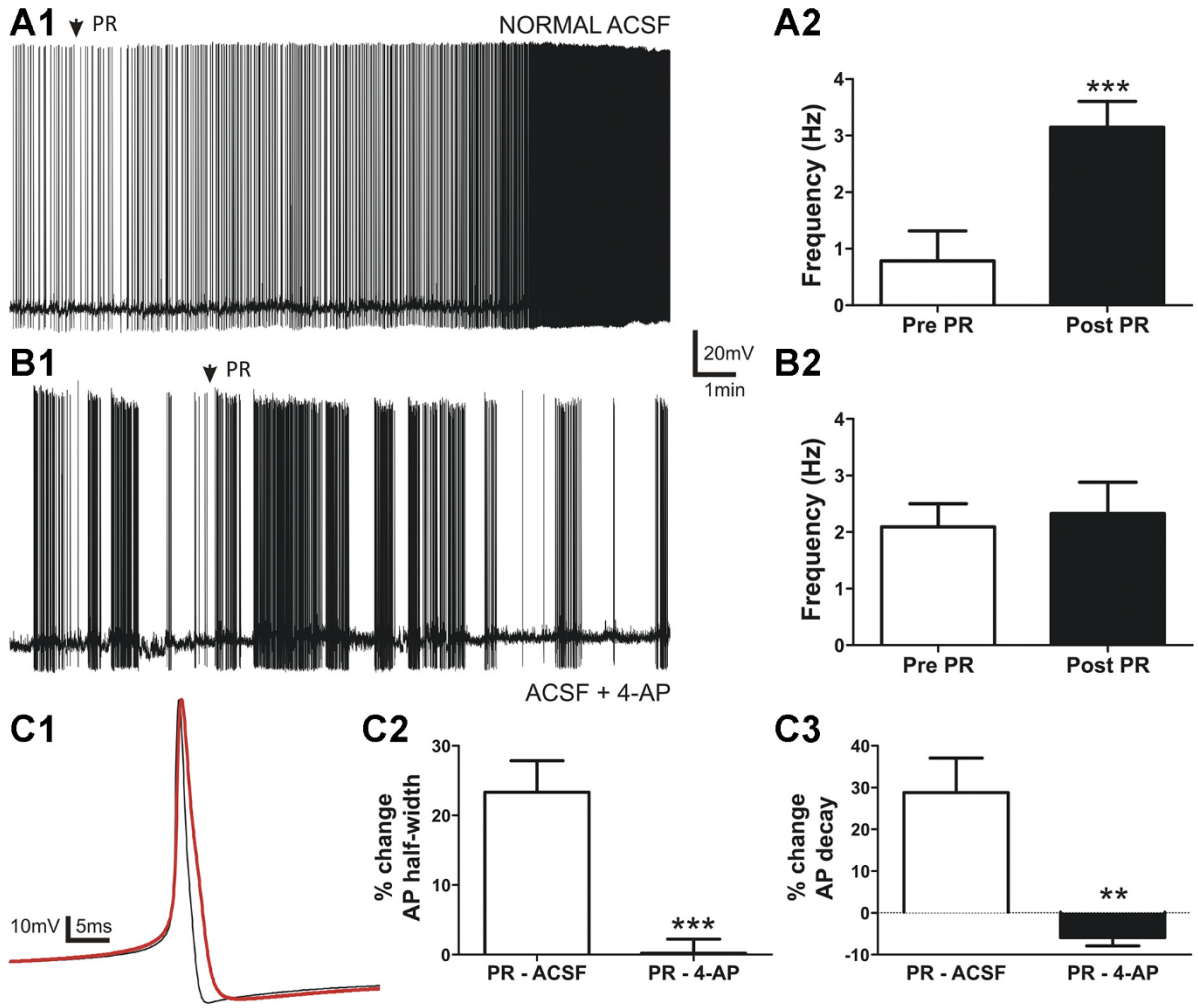

Fig. 5. The PR-mediated increase of firing frequency and changes in the action potential (AP) waveform are abolished by the I_A blocker 4-aminopyridine (4-AP). *A*,*1*: sample trace showing that PR (2.5 nM, 5 s) increased the firing discharge of VP neurons. *A*,*2*: summary data of mean firing frequency before and after PR ($n = 9$) in control artificial cerebrospinal fluid (aCSF). This excitatory effect was blocked in the presence of 4-AP (5 mM; *B*,*1*). The plot shown in *B*,*2* shows mean firing frequencies before and after PR in 4-AP ($n = 11$, 4-aminopyridine). *C*,*1*: representative examples of averaged APs before (black trace; $n = 18$) and after PR (red trace; $n = 172$) from a representative neuron in control aCSF. Note the increased half-width, slower decay time, and smaller hyperpolarizing afterpotential peak on the red trace. Plots of mean percent change of AP half-width (*C*,*2*) and decay time (*C*,*3*) after PR in normal aCSF (white; $n = 10$) and in the presence of 4-AP (black; $n = 9$) are shown. $^{***}P < 0.001$ vs. pre-PR using Student's paired *t*-test; $^{**}P < 0.01$ and $^{***}P < 0.001$ vs. PR-aCSF by unpaired *t*-test.

evidence supporting that *1*) PR inhibits the magnitude of the A-type K^+ current in a voltage-dependent manner; *2*) PR modulates I_A inactivation properties, making the rate of inactivation faster and shifting the voltage dependence of inactivation to more hyperpolarized V_m; *3*) PR inhibits the availability of a sustained I_A window current at/or near resting V_m; *4*) PR stimulation of VP neuronal firing and changes in the AP waveform are prevented by the I_A blocker 4-AP; and *5*) PR actions do not involve increased oxidative stress. Taken together, these results support the notion that PR/PRR inhibition of A-type K^+ channels plays a critical role in mediating the central actions of PR in the regulation of VP neuronal activity and hormonal release.

Prorenin modulates A-type K^+ channel properties in VP neurons. Voltage-gated K^+ currents constitute a major intrinsic mechanism by which neurons regulate membrane excitability.

Table 1. *Properties of APs before and after PR*

Extracellular Solution	*n*	AP Half-Width Before PR, ms	AP Half-Width After PR, ms	AP Decay Before PR, ms	AP Decay After PR, ms	HAP Peak Before PR, mV	HAP Peak After PR, mV
aCSF	10	1.4 ± 0.1	1.8 ± 0.1‡	0.9 ± 0.1	1.2 ± 0.1†	−16.3 ± 0.7	−14.8 ± 0.5*
aCSF + 4-aminopyridine	9	3.8 ± 0.4	3.8 ± 0.4	3.3 ± 0.3	3.1 ± 0.3*	−16.3 ± 2.2	−16.2 ± 2.2

Values are expressed as means ± SE. AP, action potential; PR, prorenin; HAP, hyperpolarizing afterpotential; decay, 90–37% decay time; half-width, half-width duration; aCSF, artificial cerebrospinal fluid. Differences were significant at $^*P < 0.05$, $^†P < 0.01$, and $^‡P < 0.001$ vs. the respective property before PR using Student's paired *t*-test.

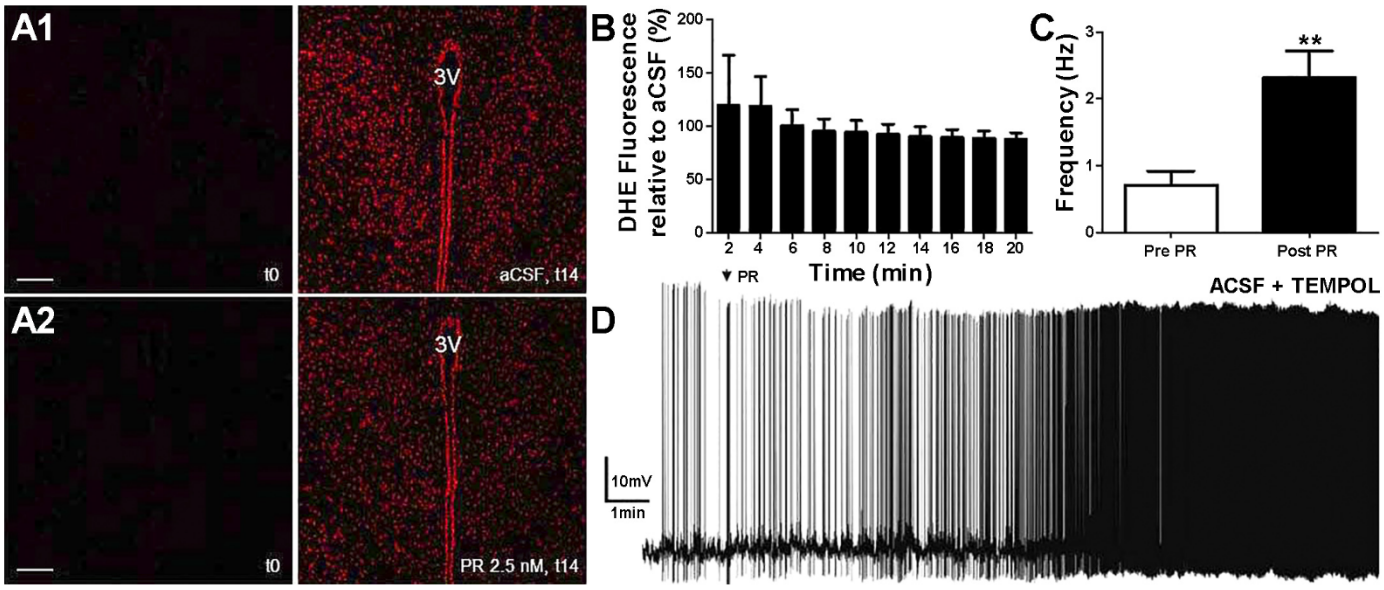

Fig. 6. PR effects on hypothalamic neurons do not involve the production of ROS. Confocal images of dihydroethidium (DHE) staining acquired at time = 0 min and 14 min in regular aCSF (*A,1*) or PR (2.5 nM; *A,2*) within paraventricular nucleus-containing slices are shown. *B*: mean data of DHE fluorescence intensity over time (obtained every 2 min, from time = 2−20 min) in PR relative to aCSF ($n = 5$ slices in each group). *C*: summary data from whole cell patch-clamp recordings showing mean firing frequencies (in Hz) before and after PR application (arrow; 5-s application) in the presence of tempol (5 mM). *D*: sample trace showing that PR excitatory effects persisted in this condition. $^{**}P < 0.01$ vs. pre-PR using Student's paired *t*-test. 3V, third ventricle. Scale bars in *A,1* and *A, 2* = 50 μm.

Among them, I_A is a transient, voltage-dependent subthreshold current that displays fast activating and inactivating kinetics. These channels are known to influence both the rate and firing pattern of VP neurons, contributing to AP repolarization and prolonging AP interspike intervals (5). Work from our laboratory has shown that I_A can be modulated by different signals, including activation of glutamate *N*-methyl-D-aspartate receptors, resulting in Ca^{2+}-dependent inhibition of I_A (31). In a recent study (34), we showed that PR-evoked excitation of VP neurons involved Ca^{2+}-dependent inhibition of K^+ current. However, the molecular identity of such a current remained to be determined. Here, we demonstrate that PR inhibited I_A magnitude in a voltage-dependent manner, with PR effects becoming greater at more depolarized V_m. This range of voltages is normally reached during AP firing, so this inhibition would be expected to have a functional impact on the firing degree of VP neurons and, consequently, systemic hormonal release (4). PR actions, however, did not involve changes in I_A voltage-dependent activation properties, as $V_{½}$ was not significantly affected after PR exposure.

Another major property of I_A is its rapid inactivation rate after channel opening upon membrane depolarization. Moreover, I_A also shows a steady-state inactivation process, which is voltage dependent and determines the number of channels available to be activated at any given voltage after membrane depolarization. Our results show that PR sped up the rate of I_A inactivation, and, more importantly, it also enhanced the degree of I_A steady-state inactivation. This is reflected by the fact that I_A steady-state inactivation curves were shifted to more negative V_m, an effect that translates into a reduced availability of these channels to be opened at any given voltage. This could be, in turn, a factor contributing to less I_A activation upon membrane depolarization, as shown in Fig. 3. This is supported by the fact that when steady-state inactivation was almost completely removed by repeating activation protocols while holding neurons at more hyperpolarized levels (i.e., starting from a holding V_m of −100 mV instead of −75 mV), the PR-mediated I_A inhibition was significantly diminished. These data are consistent with previous reports that have shown that a faster rate of inactivation and a hyperpolarizing shift of I_A steady-state inactivation correlated with enhanced neuronal excitability (37, 44, 46).

Previous studies have described the existence of a window current for I_A in magnocellular and presympathetic neurons of the hypothalamus (5, 46). This window current is due to a partial activation and incomplete inactivation of a proportion of A-type K^+ channels, resulting in a sustained I_A spanning over a physiologically relevant range of V_m. Importantly, since VP neurons are electrotonically compact and have a high input resistance (48), this small window current could have significant effects on V_m. Our results show that PR inhibited this window current around resting potentials, shifting its range to more hyperpolarized voltages. Inhibition of this sustained window current thus likely contributed to membrane depolarization and increased firing discharge mediated by PR (see more below).

Contribution of I_A to PR effects on the AP waveform and firing discharge. As mentioned above, I_A regulates both repetitive firing properties and single AP waveform in different cell types (25, 28, 46). Here, we show that the PR-mediated increase in firing activity and on the AP waveform (wider and slower decaying APs) was prevented when slices were exposed to the I_A channel blocker 4-AP, suggesting that PR-evoked excitatory effects were at least in part mediated by I_A inhibition. It is worth noting that the basal firing frequency of neurons preincubated with 4-AP was higher than that of neurons in control conditions, results consistent with previous reports showing that 4-AP (1–5

mM) depolarized hypothalamic neurons, increasing their firing discharge (5, 46). Still, the increase in firing rate evoked by PR in control conditions was higher than that evoked by 4-AP alone (i.e., 3 vs. 2 Hz), suggesting that PR may be acting also via a non-I_A-mediated mechanism. Another caveat regarding these results is that the occlusion of the PR effect by 4-AP could be due to a "ceiling" effect. However, the fact that the firing frequency of neurons in the presence of 4-AP was below the maximum frequency attained in control conditions would argue against a ceiling effect. Still, 4-AP effects on the AP waveform were substantially larger than those evoked by PR, which could have prevented any further effect by the latter on the action potential waveform. Even if this were the case, we believe that the effect of PR on firing activity was not secondary to the changes in the AP waveform. In fact, slowing down of the action potential per se would be expected to have the opposite effect on firing frequency.

Thus, taken together, our results indicate that by affecting the resting V_m and repetitive firing properties, inhibition of A-type K^+ channels plays a major role in mediating effects of PR/PRR on VP excitability and hormonal release.

Potential mechanisms underlying PR-mediated I_A inhibition of VP neurons. The precise underlying mechanisms by which PR leads to changes in A-type K^+ channel function are still unknown. Although not tested again in this study, we recently reported that PR effects on VP neurons occurred in an ANG II-independent manner, involving direct intracellular cascades and increases in intracellular Ca^{2+} levels, after activation of PRR (34). PRR is known to be coupled to different signaling pathways, including MAPK and ERK1/2 (13, 18, 39). These signaling cascades could lead, in turn, to a Ca^{2+}-dependent change in the balance of kinase/phosphatase activity. Importantly, the voltage-dependent properties of A-type K^+ channels, particularly inactivation, are highly dependent on the phosphorylation state of the channels (36). Still, whether a Ca^{2+}-dependent phosphorylation of A-type K^+ channels contributes to PR/PRR inhibition of I_A in VP neurons remains to be determined.

PR/PRR effects have also been associated with intracellular signaling pathways leading to the generation of ROS (19, 33). Moreover, oxidative stress has been shown to decrease K^+ channel activity (27, 50). These pieces of evidence led us to hypothesize that PR-mediated effects on VP neurons involved ROS production. However, our electrophysiological experiments showing that PR excitatory effects persisted in the presence of the SOD mimetic tempol, along with our DHE imaging experiment showing lack of in situ ROS generation (3) by PR, argue against the contribution of oxidative stress to PR-mediated effects on VP neural activity. These results are somewhat in disagreement with the studies mentioned above. However, it is important to note that those experiments were not performed in hypothalamic slices but rather in neuronal cultures and using higher concentrations of PR (100 vs. 2.5–5 nM) and with longer incubation times (1 h vs. 20 min). An important caveat of the DHE experiments, however, is that the profiles randomly selected for quantification were not phenotypically identified and may include neurons as well as glial cells.

Perspectives

Understanding the precise cellular pathways and neurobiological mechanisms by which the RAS regulates cardiovascular function is critical in the search of novel therapeutic targets for the treatment of cardiovascular disease. Although the roles of the peripheral RAS are well established, there is still an ongoing debate related to the contribution and mechanisms by which the central RAS influences cardiovascular control (43, 52). For example, all RAS components are expressed in the SON and PVN (29), as well as ANG II and AT_1Rs, have been proposed as key players underlying RAS-mediated increases in sympathoexcitatory outflow and VP systemic release (24, 35, 42, 53). However, recent studies have provided evidence for the lack of AT_1Rs and ANG II type 2 receptors on presympathetic and VP cells (9–11), whereas others have supported the contribution of astroglial cells as alternative cellular targets mediating central ANG II actions in these neuronal populations (3, 49).

In addition to ANG II and its receptors, PR and PRR have recently emerged as two of the most novel players of the central RAS involved in the regulation of sympathetic and neurosecretory outflows from the hypothalamus (19, 32, 41). Indeed, a recent study from our laboratory confirmed the expression of PRR on these neurons and show that their activation efficiently modulates their firing activity (34). The present study further corroborates the importance of the PR/PRR signaling pathway as key components of the central RAS involved in the modulation of VP neuronal activity and identified A-type K^+ channels as key underlying molecular targets.

Finally, a growing body of evidence indicates that an elevated PR/PRR expression and function in the hypothalamus contributes to high blood pressure and enhanced systemic release of VP (19, 41). Moreover, diminished I_A expression/function has been reported as an underlying mechanism leading to increased hypothalamic neuronal excitability during hypertension (2, 44, 45). Thus, future studies are warranted to determine whether enhanced PR/PRR signaling within the SON/PVN contributes to blunted I_A function, exacerbated VP neuronal activity, and, consequently, elevated systemic release of VP during hypertension.

ACKNOWLEDGMENTS

The authors thank Dr. Vinicia C. Biancardi (of Auburn University) for the kind assistance with the dihydroethidium experiments used in this study.

GRANTS

This work was supported by National Heart, Lung, and Blood Institute Grant R01-HL-112225 (to J. E. Stern).

DISCLOSURES

No conflicts of interest, financial or otherwise, are declared by the authors.

AUTHOR CONTRIBUTIONS

S.P. and J.E.S. conceived and designed research; S.P. performed experiments; S.P. analyzed data; S.P. and J.E.S. interpreted results of experiments; S.P. prepared figures; S.P. and J.E.S. drafted manuscript; S.P. and J.E.S. edited and revised manuscript; S.P. and J.E.S. approved final version of manuscript.

REFERENCES

1. **Armstrong WE, Smith BN, Tian M.** Electrophysiological characteristics of immunochemically identified rat oxytocin and vasopressin neurones in vitro. *J Physiol* 475: 115–128, 1994. doi:10.1113/jphysiol.1994.sp020053.

2. **Belugin S, Mifflin S.** Transient voltage-dependent potassium currents are reduced in NTS neurons isolated from renal wrap hypertensive rats. *J Neurophysiol* 94: 3849–3859, 2005. doi:10.1152/jn.00573.2005.
3. **Biancardi VC, Stranahan AM, Krause EG, de Kloet AD, Stern JE.** Cross talk between AT_1 receptors and Toll-like receptor 4 in microglia contributes to angiotensin II-derived ROS production in the hypothalamic paraventricular nucleus. *Am J Physiol Heart Circ Physiol* 310: H404–H415, 2016. doi:10.1152/ajpheart.00247.2015.
4. **Bourque CW.** Intraterminal recordings from the rat neurohypophysis in vitro. *J Physiol* 421: 247–262, 1990. doi:10.1113/jphysiol.1990.sp017943.
5. **Bourque CW.** Transient calcium-dependent potassium current in magnocellular neurosecretory cells of the rat supraoptic nucleus. *J Physiol* 397: 331–347, 1988. doi:10.1113/jphysiol.1988.sp017004.
6. **Cazalis M, Dayanithi G, Nordmann JJ.** The role of patterned burst and interburst interval on the excitation-coupling mechanism in the isolated rat neural lobe. *J Physiol* 369: 45–60, 1985. doi:10.1113/jphysiol.1985.sp015887.
7. **Chevalier M, Lory P, Mironneau C, Macrez N, Quignard JF.** T-type CaV3.3 calcium channels produce spontaneous low-threshold action potentials and intracellular calcium oscillations. *Eur J Neurosci* 23: 2321–2329, 2006. doi:10.1111/j.1460-9568.2006.04761.x.
8. **Dampney RA.** Functional organization of central pathways regulating the cardiovascular system. *Physiol Rev* 74: 323–364, 1994.
9. **de Kloet AD, Pati D, Wang L, Hiller H, Sumners C, Frazier CJ, Seeley RJ, Herman JP, Woods SC, Krause EG.** Angiotensin type 1a receptors in the paraventricular nucleus of the hypothalamus protect against diet-induced obesity. *J Neurosci* 33: 4825–4833, 2013. doi:10.1523/JNEUROSCI.3806-12.2013.
10. **de Kloet AD, Pitra S, Wang L, Hiller H, Pioquinto DJ, Smith JA, Sumners C, Stern JE, Krause EG.** Angiotensin type-2 receptors influence the activity of vasopressin neurons in the paraventricular nucleus of the hypothalamus in male mice. *Endocrinology* 157: 3167–3180, 2016. doi:10.1210/en.2016-1131.
11. **de Kloet AD, Wang L, Pitra S, Hiller H, Smith JA, Tan Y, Nguyen D, Cahill KM, Sumners C, Stern JE, Krause EG.** A unique "angiotensin-sensitive" neuronal population coordinates neuroendocrine, cardiovascular, and behavioral responses to stress. *J Neurosci* 37: 3478–3490, 2017. doi:10.1523/JNEUROSCI.3674-16.2017.
12. **Dzau VJ.** Circulating versus local renin-angiotensin system in cardiovascular homeostasis. *Circulation* 77: I4–I13, 1988.
13. **Feldt S, Batenburg WW, Mazak I, Maschke U, Wellner M, Kvakan H, Dechend R, Fiebeler A, Burckle C, Contrepas A, Jan Danser AH, Bader M, Nguyen G, Luft FC, Muller DN.** Prorenin and renin-induced extracellular signal-regulated kinase 1/2 activation in monocytes is not blocked by aliskiren or the handle-region peptide. *Hypertension* 51: 682–688, 2008. doi:10.1161/HYPERTENSIONAHA.107.101444.
14. **Fisher TE, Voisin DL, Bourque CW.** Density of transient K^+ current influences excitability in acutely isolated vasopressin and oxytocin neurones of rat hypothalamus. *J Physiol* 511: 423–432, 1998. doi:10.1111/j.1469-7793.1998.423bh.x.
15. **Flores-Hernández J, Galarraga E, Pineda JC, Bargas J.** Patterns of excitatory and inhibitory synaptic transmission in the rat neostriatum as revealed by 4-AP. *J Neurophysiol* 72: 2246–2256, 1994.
16. **Guyenet PG.** The sympathetic control of blood pressure. *Nat Rev Neurosci* 7: 335–346, 2006. doi:10.1038/nrn1902.
17. **Hall JE.** Historical perspective of the renin-angiotensin system. *Mol Biotechnol* 24: 27–39, 2003. doi:10.1385/MB:24:1:27.
18. **Huang Y, Wongamorntham S, Kasting J, McQuillan D, Owens RT, Yu L, Noble NA, Border W.** Renin increases mesangial cell transforming growth factor-β_1 and matrix proteins through receptor-mediated, angiotensin II-independent mechanisms. *Kidney Int* 69: 105–113, 2006. doi:10.1038/sj.ki.5000011.
19. **Huber MJ, Basu R, Cecchettini C, Cuadra AE, Chen QH, Shan Z.** Activation of the (pro)renin receptor in the paraventricular nucleus increases sympathetic outflow in anesthetized rats. *Am J Physiol Heart Circ Physiol* 309: H880–H887, 2015. doi:10.1152/ajpheart.00095.2015.
20. **Jackson K, Silva HM, Zhang W, Michelini LC, Stern JE.** Exercise training differentially affects intrinsic excitability of autonomic and neuroendocrine neurons in the hypothalamic paraventricular nucleus. *J Neurophysiol* 94: 3211–3220, 2005. doi:10.1152/jn.00277.2005.
21. **Li W, Peng H, Cao T, Sato R, McDaniels SJ, Kobori H, Navar LG, Feng Y.** Brain-targeted (pro)renin receptor knockdown attenuates angiotensin II-dependent hypertension. *Hypertension* 59: 1188–1194, 2012. doi:10.1161/HYPERTENSIONAHA.111.190108.
22. **Li W, Peng H, Mehaffey EP, Kimball CD, Grobe JL, van Gool JM, Sullivan MN, Earley S, Danser AH, Ichihara A, Feng Y.** Neuron-specific (pro)renin receptor knockout prevents the development of salt-sensitive hypertension. *Hypertension* 63: 316–323, 2014. doi:10.1161/HYPERTENSIONAHA.113.02041.
23. **Li W, Peng H, Seth DM, Feng Y.** The prorenin and (pro)renin receptor: new players in the brain renin-angiotensin system? *Int J Hypertens* 2012: 290635, 2012. doi:10.1155/2012/290635.
24. **Li YF, Wang W, Mayhan WG, Patel KP.** Angiotensin-mediated increase in renal sympathetic nerve discharge within the PVN: role of nitric oxide. *Am J Physiol Regul Integr Comp Physiol* 290: R1035–R1043, 2006. doi:10.1152/ajpregu.00338.2004.
25. **Li Z, Ferguson AV.** Electrophysiological properties of paraventricular magnocellular neurons in rat brain slices: modulation of I_A by angiotensin II. *Neuroscience* 71: 133–145, 1996. doi:10.1016/0306-4522(95)00434-3.
26. **Li Z, Ji G, Neugebauer V.** Mitochondrial reactive oxygen species are activated by mGluR5 through IP_3 and activate ERK and PKA to increase excitability of amygdala neurons and pain behavior. *J Neurosci* 31: 1114–1127, 2011. doi:10.1523/JNEUROSCI.5387-10.2011.
27. **Liu Y, Gutterman DD.** Oxidative stress and potassium channel function. *Clin Exp Pharmacol Physiol* 29: 305–311, 2002. doi:10.1046/j.1440-1681.2002.03649.x.
28. **Luther JA, Tasker JG.** Voltage-gated currents distinguish parvocellular from magnocellular neurones in the rat hypothalamic paraventricular nucleus. *J Physiol* 523: 193–209, 2000. doi:10.1111/j.1469-7793.2000.t01-1-00193.x.
29. **McKinley MJ, Albiston AL, Allen AM, Mathai ML, May CN, McAllen RM, Oldfield BJ, Mendelsohn FA, Chai SY.** The brain renin-angiotensin system: location and physiological roles. *Int J Biochem Cell Biol* 35: 901–918, 2003. doi:10.1016/S1357-2725(02)00306-0.
30. **Molineux ML, Fernandez FR, Mehaffey WH, Turner RW.** A-type and T-type currents interact to produce a novel spike latency-voltage relationship in cerebellar stellate cells. *J Neurosci* 25: 10863–10873, 2005. doi:10.1523/JNEUROSCI.3436-05.2005.
31. **Naskar K, Stern JE.** A functional coupling between extrasynaptic NMDA receptors and A-type K^+ channels under astrocyte control regulates hypothalamic neurosecretory neuronal activity. *J Physiol* 592: 2813–2827, 2014. doi:10.1113/jphysiol.2014.270793.
32. **Nguyen G, Delarue F, Burcklé C, Bouzhir L, Giller T, Sraer JD.** Pivotal role of the renin/prorenin receptor in angiotensin II production and cellular responses to renin. *J Clin Invest* 109: 1417–1427, 2002. doi:10.1172/JCI0214276.
33. **Peng H, Li W, Seth DM, Nair AR, Francis J, Feng Y.** (Pro)renin receptor mediates both angiotensin II-dependent and -independent oxidative stress in neuronal cells. *PLoS One* 8: e58339, 2013. doi:10.1371/journal.pone.0058339.
34. **Pitra S, Feng Y, Stern JE.** Mechanisms underlying prorenin actions on hypothalamic neurons implicated in cardiometabolic control. *Mol Metab* 5: 858–868, 2016. doi:10.1016/j.molmet.2016.07.010.
35. **Polson JW, Dampney RA, Boscan P, Pickering AE, Paton JF.** Differential baroreflex control of sympathetic drive by angiotensin II in the nucleus tractus solitarii. *Am J Physiol Regul Integr Comp Physiol* 293: R1954–R1960, 2007. doi:10.1152/ajpregu.00041.2007.
36. **Ritter DM, Ho C, O'Leary ME, Covarrubias M.** Modulation of Kv3.4 channel N-type inactivation by protein kinase C shapes the action potential in dorsal root ganglion neurons. *J Physiol* 590: 145–161, 2012. doi:10.1113/jphysiol.2011.218560.
37. **Robertson WP, Schofield GG.** Primary and adaptive changes of A-type K^+ currents in sympathetic neurons from hypertensive rats. *Am J Physiol Regul Integr Comp Physiol* 276: R1758–R1765, 1999.
38. **Romero CA, Orias M, Weir MR.** Novel RAAS agonists and antagonists: clinical applications and controversies. *Nat Rev Endocrinol* 11: 242–252, 2015. doi:10.1038/nrendo.2015.6.
39. **Sakoda M, Ichihara A, Kaneshiro Y, Takemitsu T, Nakazato Y, Nabi AH, Nakagawa T, Suzuki F, Inagami T, Itoh H.** (Pro)renin receptor-mediated activation of mitogen-activated protein kinases in human vascular smooth muscle cells. *Hypertens Res* 30: 1139–1146, 2007. doi:10.1291/hypres.30.1139.
40. **Shan Z, Cuadra AE, Sumners C, Raizada MK.** Characterization of a functional (pro)renin receptor in rat brain neurons. *Exp Physiol* 93: 701–708, 2008. doi:10.1113/expphysiol.2008.041988.
41. **Shan Z, Shi P, Cuadra AE, Dong Y, Lamont GJ, Li Q, Seth DM, Navar LG, Katovich MJ, Sumners C, Raizada MK.** Involvement of the

brain (pro)renin receptor in cardiovascular homeostasis. *Circ Res* 107: 934–938, 2010. doi:10.1161/CIRCRESAHA.110.226977.

42. **Shoji M, Share L, Crofton JT, Brooks DP.** The effect on vasopressin release of microinjection of cholinergic agonists into the paraventricular nucleus of conscious rats. *J Neuroendocrinol* 1: 401–406, 1989. doi:10.1111/j.1365-2826.1989.tb00138.x.
43. **Sigmund CD, Diz DI, Chappell MC.** No brain renin-angiotensin system: déjà vu all over again? *Hypertension* 69: 1007–1010, 2017. doi:10.1161/HYPERTENSIONAHA.117.09167.
44. **Sonner PM, Filosa JA, Stern JE.** Diminished A-type potassium current and altered firing properties in presympathetic PVN neurones in renovascular hypertensive rats. *J Physiol* 586: 1605–1622, 2008. doi:10.1113/jphysiol.2007.147413.
45. **Sonner PM, Lee S, Ryu PD, Lee SY, Stern JE.** Imbalanced K^+ and Ca^{2+} subthreshold interactions contribute to increased hypothalamic presympathetic neuronal excitability in hypertensive rats. *J Physiol* 589: 667–683, 2011. doi:10.1113/jphysiol.2010.198556.
46. **Sonner PM, Stern JE.** Functional role of A-type potassium currents in rat presympathetic PVN neurones. *J Physiol* 582: 1219–1238, 2007. doi:10.1113/jphysiol.2007.134379.
47. **Stern JE, Armstrong WE.** Electrophysiological differences between oxytocin and vasopressin neurones recorded from female rats in vitro. *J Physiol* 488: 701–708, 1995. doi:10.1113/jphysiol.1995.sp021001.
48. **Stern JE, Armstrong WE.** Reorganization of the dendritic trees of oxytocin and vasopressin neurons of the rat supraoptic nucleus during lactation. *J Neurosci* 18: 841–853, 1998.
49. **Stern JE, Son S, Biancardi VC, Zheng H, Sharma N, Patel KP.** Astrocytes contribute to angiotensin II stimulation of hypothalamic neuronal activity and sympathetic outflow. *Hypertension* 68: 1483–1493, 2016. doi:10.1161/HYPERTENSIONAHA.116.07747.
50. **Sun C, Sellers KW, Sumners C, Raizada MK.** NAD(P)H oxidase inhibition attenuates neuronal chronotropic actions of angiotensin II. *Circ Res* 96: 659–666, 2005. doi:10.1161/01.RES.0000161257.02571.4b.
51. **Ueta Y, Fujihara H, Serino R, Dayanithi G, Ozawa H, Matsuda K, Kawata M, Yamada J, Ueno S, Fukuda A, Murphy D.** Transgenic expression of enhanced green fluorescent protein enables direct visualization for physiological studies of vasopressin neurons and isolated nerve terminals of the rat. *Endocrinology* 146: 406–413, 2005. doi:10.1210/en.2004-0830.
52. **van Thiel BS, Góes Martini A, Te Riet L, Severs D, Uijl E, Garrelds IM, Leijten FPJ, van der Pluijm I, Essers J, Qadri F, Alenina N, Bader M, Paulis L, Rajkovicova R, Domenig O, Poglitsch M, Danser AH.** Brain renin-angiotensin system: does it exist? *Hypertension* 69: 1136–1144, 2017. doi:10.1161/HYPERTENSIONAHA.116.08922.
53. **Wei SG, Yu Y, Zhang ZH, Felder RB.** Angiotensin II upregulates hypothalamic AT_1 receptor expression in rats via the mitogen-activated protein kinase pathway. *Am J Physiol Heart Circ Physiol* 296: H1425–H1433, 2009. doi:10.1152/ajpheart.00942.2008.
54. **Yin JX, Yang RF, Li S, Renshaw AO, Li YL, Schultz HD, Zimmerman MC.** Mitochondria-produced superoxide mediates angiotensin II-induced inhibition of neuronal potassium current. *Am J Physiol Cell Physiol* 298: C857–C865, 2010. doi:10.1152/ajpcell.00313.2009.
55. **Zhang ZH, Yu Y, Kang YM, Wei SG, Felder RB.** Aldosterone acts centrally to increase brain renin-angiotensin system activity and oxidative stress in normal rats. *Am J Physiol Heart Circ Physiol* 294: H1067–H1074, 2008. doi:10.1152/ajpheart.01131.2007.